# Sudden-Discharging Quench Dynamics in a No-Insulation Superconducting Coil

Fangliang Dong, Dongkeun Park*, Junseong Kim, Juan Bascuñán, and Yukikazu Iwasa

***Abstract*—It is generally agreed that no-insulation (NI) high-temperature superconducting (HTS) magnets do not quench because of the turn-to-turn energy-releasing bypass unique to NI. However, these magnets, especially with high operating current and low ambient thermal capacity, still occur unexpected quenches when the current through the magnets suddenly drops to zero (i.e., the sudden-discharging quench). Here, we report this kind of quench, which is different from that widely-reported quench happening during charging (i.e., the energizing quench). Here, a demonstrative coil with 655-turns, 350 A operating current, and 4 K conduction cooling, is used to prove this sudden-discharging quench, and a simulation model is built to reveal the quench dynamics. Results show the turn-to-turn heat triggers the initial partial quench in the inner coil turns and then the induced overcurrent spreads out the quench like an avalanche to the outer coil turns.**

***Index Terms*—HTS magnet; No-insulation; Quench.**

## I. Introduction

The enhanced self-protecting ability of no-insulation (NI) second-generation (2G) high-temperature superconducting (HTS) magnets has been demonstrated experimentally compared to insulted counterparts. The key idea of the NI technique is to completely eliminate turn-to-turn insulation within the HTS winding [1]. In the event of a quench, it is confirmed that the magnet current in an NI winding can automatically bypass the quench spot through radial turn-to-turn contacts from its original spiral path [2-4], and that the magnet remains stable even though its operating current is pushed to twice the magnet critical current [1]. Due to this self-protecting feature, the absence of turn-to-turn insulation and extra tape stabilizer needed in an insulated magnet now can be both eliminated, making the NI magnet highly compact [5-8] with larger overall current density. Both the features of self-protecting and high current density (>150 kA/cm$^2$) [9] are unachievable with the conventional HTS magnet, therefore, the NI technique is becoming a promising candidate for various applications like electrical motors [10-12], high-field physics [13, 14], and biotechnology [15, 16], etc.

Manuscript receipt and acceptance dates will be inserted here. This work was supported by National Institute of General Medical Sciences of the National Institutes of Health (Project No. R01GM137138). *(Corresponding author: Dongkeun Park)*

All of the authors are with the Francis Bitter Magnet Laboratory/Plasma Science and Fusion Center, Massachusetts Institute of Technology, Cambridge, MA 02139, USA (e-mail: dk_park@mit.edu).

Color versions of one or more of the figures in this paper are available online at http://IEEExplore.IEEE.org.

Digital Object Identifier will be inserted here upon acceptance.

However, during our development programs on magnets, we experienced quenches even if the NI winding technique can be immune to some in-coil defects. Different from the widely-reported quench during energizing [17, 18] that usually occurs because of magnet internal defects, our reported quench happens when the current through the magnets suddenly drops to zero (that is, the sudden discharging). The energizing quench has a chance to be avoided by proper designs [19-22], while the sudden-discharging quench reported here usually appears during normal running due to unexpected external defects like electrode damages or power supply failures, which are usually unavoidable and can happen almost at any time even in well-operated and non-defective NI magnets. Especially, to attain a higher field, NI magnets are put to run at high operating current and low temperature. The large stored energy and limited thermal margin make the quench due to sudden discharge highly possible.

The sudden absence of magnetic field in NI magnets during the quench causes rapidly transient electrical and mechanical fluctuations in the winding because the coils are electromagnetically coupled. These fluctuations even lead to irreversible damages, like our previous three-nested-coil 18.8-T NI HTS magnet was mechanically damaged because of the unbalanced force and excessive hoop stresses during the quench [23, 24]. Therefore, we believe there are some issues with sudden-discharging quench in NI HTS magnets that must be resolved for this otherwise promising NI winding technique. As the start of the exploration, here we focus on the dynamics of the sudden-discharging quench, in order to provide a possible basic understanding of the quench mechanisms for a future proposition of preventive approaches.

This paper is organized as below: 1) reproduce the sudden-discharging quench through a demonstrative coil; 2) reveal the quench dynamics including electrometric, thermal, and mechanical behaviors inside the winding; 3) provide preliminary quench preventive approaches as our future work.

## II. Sudden-Discharging Quench and Simulation Model

### A. Reproduction of the Quench

The specifications of the demonstrative coil used to reproduce the sudden-discharging quench are listed in Table I. The coil is energized to 350 A and then suddenly discharged by cutting off the power supply current with a knife switch after

Template version 8.0d, 22 August 2017. IEEE will put copyright information in this area
See http://www.IEEE.org/publications_standards/publications/rights/index.html for more information.

the coil magnetic field and temperature settlement. The center magnetic field, which can represent the coil transport current, is recorded in Fig. 1. Compared to the expected discharging time constant of 4.37 s (i.e., 20.9 mH / 4.78 mΩ), the quench dropped the center field to zero within only 450 ms, as the red solid line shows in the figure.

TABLE I
SPECIFICATIONS OF THE DEMONSTRATIVE COIL

| | |
|---|---|
| HTS tape thickness / wideness | REBCO, 65 μm / 6 mm |
| Coil type | Single pancake |
| Number of turns | 655 |
| Inner / outer diameters | 19.0 / 107.4 mm |
| Inductance | 20.9 mH |
| Turn-to-turn contact resistance | 4.78 mΩ |
| Cooling | ~4.2 K conduction cooling |
| Estimated coil critical current | ~1500 A @ 4.2 K (self-field) |
| Operation mode | Driven mode |

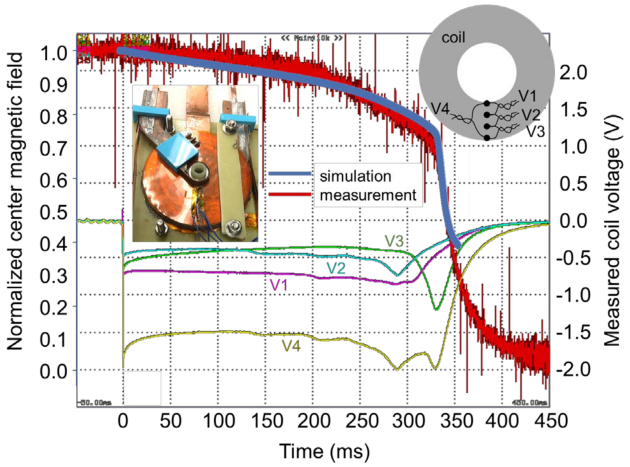


Fig. 1. Center magnetic field and coil voltages in the sudden-discharging quench. The photo in the figure is the demonstrative coil.

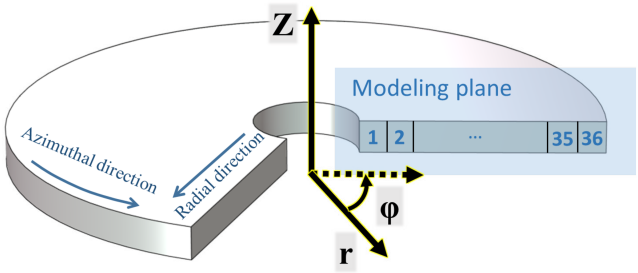


Fig. 2. The simulation model. To take advantage of the circular symmetry, the coil is built in 2D form.

### B. Simulation Model

The model couples electromagnetic, thermal, and mechanical considerations. Where the electromagnetic subsection based on the *H*-formulation originally for insulated coils [25], is modified to account for the radial turn-to-turn current flow unique in NI coils by using the "rotated anisotropic resistivity [26]". Combined with the homogenization method [27], the simulation model is built as that shown in Fig. 2. We divided the cross-sectional winding area into 36 parts for revealing the quench dynamics, while all of the physical variables are continuous in actuality. The simulated result on the overall transient behavior of the center magnetic field decay has shown in Fig. 1: we considered the simulation (the blue solid line) is in good agreement with the measurement (the red solid line), and confirmed the simulation is trustable.

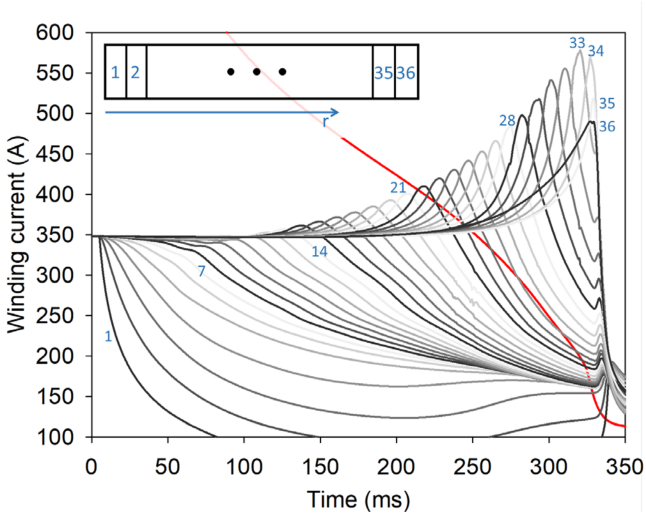


Fig. 3. The electromagnetic behavior during the quench. Monochromatic lines: coil current in each winding part; red line: average coil critical current.

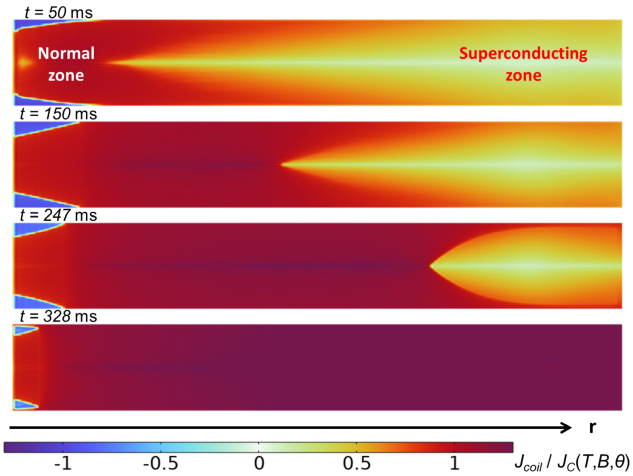


Fig. 4. The quench distributions inside the coil winding. $J_{coil}$: the winding current density; $J_C(T,B,\theta)$: the local temperature- and field-dependent critical current density.

## III. SUDDEN-DISCHARGING QUENCH DYNAMICS

With the aforementioned model, the quench behaviors in this part are revealed.

### A. Electromagnetic Behaviors

The changes on coil current in each winding part during the quench are shown in Fig. 3. The power supply is cut off at $t$ = 5 ms, then current in the innermost winding (i.e., in part 1) starts to decay first because of the lowest winding inductance. As time elapses, the currents in the rest winding parts decay in sequence (i.e., the monochromatic lines in the figure), while at around $t \approx 130$ ms, the winding current increases even over the initial current 350 A due to flux conservation and electromagnetic coupling. At $t \approx 230$ ms, the quench gradually forms

roughly from winding part 21, as the coil critical current (the red solid line) has decreased lower than the winding current. After this time point, the currents in winding parts 22 to 36 have higher and higher induced overcurrent peaks spreading like an avalanche, which are regarded as quench propagation - this phenomenon is also reflected by the sequential fluctuations on the measured voltages shown in Fig. 1 (i.e., V1, V2, and V3). The propagating speed increases towards the outermost winding part, and finally, the entire coil quenches at $t \approx$ 340 ms, as the coil critical current is lower than all of the transport currents in each winding part. The average radial quench propagation speed is 0.17 m/s.

To observe the quench distributions inside the winding, we selected four typical time points to show in Fig. 4 the ratio of winding transport current density ($J_{coil}$) to the local temperature $T$- and anisotropic field $\theta$-$B$-dependent critical current density ($J_C(T,B,\theta)$). The areas with $J_{coil}$ / $J_C(T,B,\theta)$ >1 mean quenches (i.e., the normal zones). As can be seen in the figure, the normal zone (i.e., the darker area) gradually squeezes the superconducting zone (i.e., the lighter area) to the outer winding part. At last, the normal zone fills out of the overall winding area, developing the partial quench gradually to the entire quench.

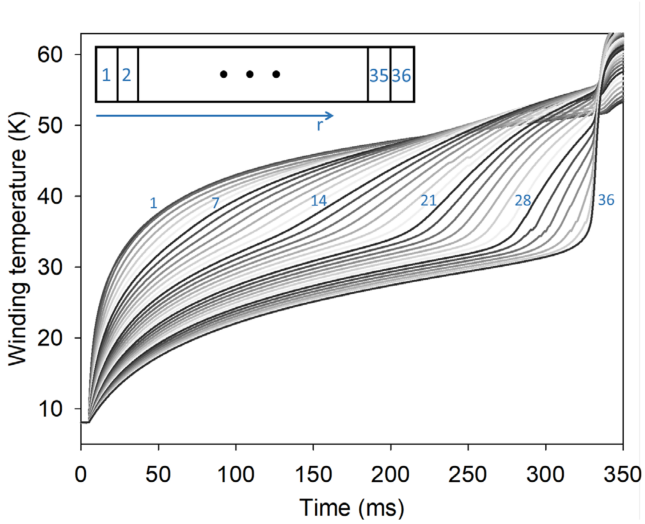


Fig. 5. The temperature changes in each winding part during the quench.

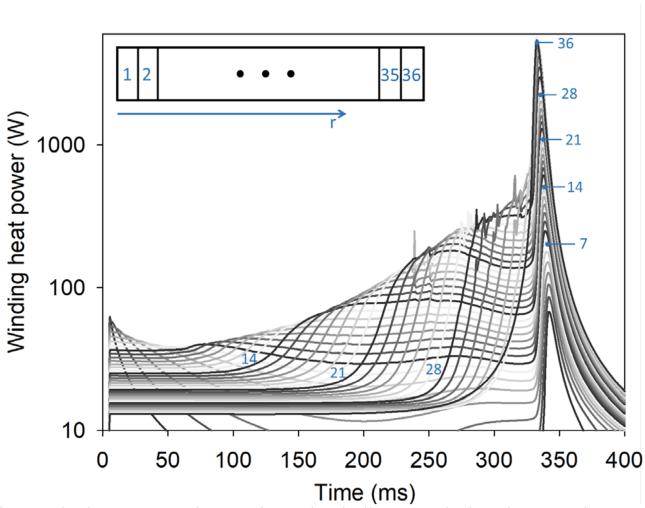


Fig. 6. The heat power changes in each winding part during the quench.

## B. *Thermal Behaviors*

Fig. 5 shows the temperature changes in the winding. Due to the initial transport current dropping in the inner winding parts, the temperature also first rises in these parts by local turn-to-turn heat. As heat diffuses, the following winding parts are heated in sequence, causing the corresponding critical currents of the winding part to drop close to the transport currents. We can refer that the local turn-to-turn heat in the winding, acting like a heat source caused by the turn-to-turn bypassing current, triggers the initial partial quench. However, the temperature rise is not rapid until the entire quench at $t \approx$ 340 ms - this indicates that the quench propagation is not mainly led by heat diffusion.

Fig. 6 is the generated heat power in each winding part during the quench, which contains turn-to-turn heat and superconducting quench heat. The heat power rapidly increases exactly at the moment when the entire coil quenches, explaining the sudden rising of winding temperature. Meanwhile, the outer winding parts have higher power peaks compared to those of inner winding parts - just appear with similar fluctuations as the induced overcurrent peaks shown in Fig. 3 (i.e., generally, outer winding parts have higher fluctuation peaks).

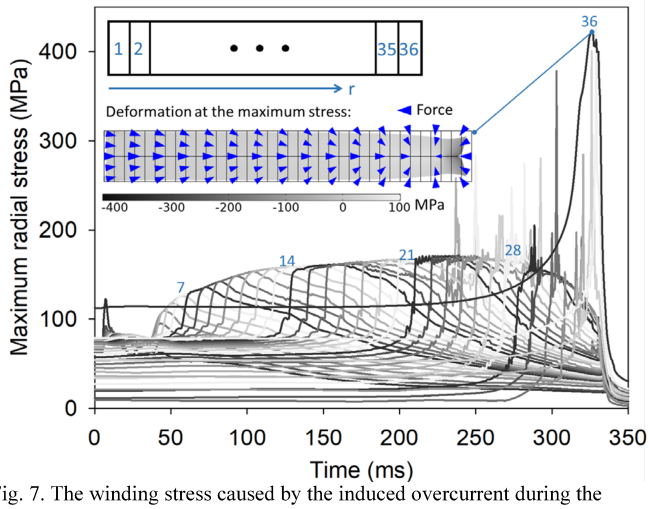


Fig. 7. The winding stress caused by the induced overcurrent during the quench.

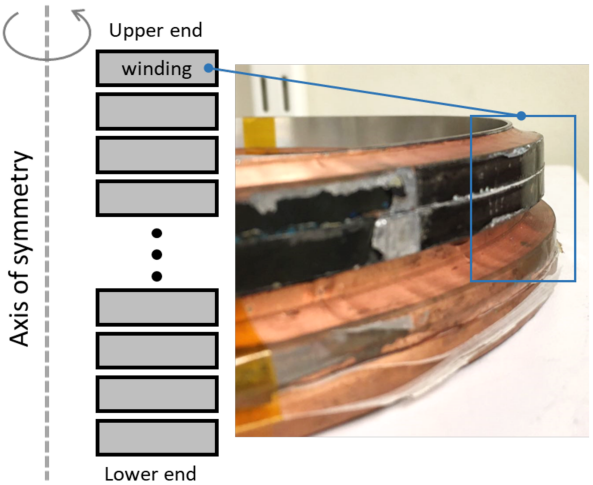


Fig. 8. Deformation of the outer winding part due to electromagnetic forces during the quench.

### C. Mechanical Behaviors

The unbalanced hoop stress is considered chiefly from the induced overcurrent. As can be seen in Fig. 7, the maximum stress happens in the outer winding parts when the entire coil quenches at $t \approx 340$ ms, this is generally in accordance with the happening time of the highest induced overcurrent in the winding. We also show in the figure the deformation of the winding at the moment when happens the maximum stress. The outer winding part tends to shrink under electromagnetic forces due to the overcurrent [28]. In a full-scale magnet consisting of many pancake coils, this force would deform the outer winding parts in the end coils and consequently destroy the magnet, as shown in Fig. 8.

### D. Possible Quench Preventive Approach

We consider an external shunt resistor [29] would provide an extra path to extract a certain portion of the transport current in the coil when happens sudden discharging. Therefore, initial turn-to-turn heat can be suppressed, and its role as a quench initiator can also be eliminated. The shunt resistor, preliminarily designed to connect across the two coil terminals, needs optimization according to, for example, instantaneous coil cooling performance, inductance, and turn-to-turn resistance, because too large resistance would weaken the quench preventive effect, while too small resistance would lead to a long changing delay.

## IV. Conclusion

We report a sudden-discharging quench in a no-insulation coil, which can happen almost at any time due to external failures. The dynamics of this quench are summarized as the turn-to-turn heat triggers the initial partial quench in the inner coil turns, then the quench is spread out by induced overcurrent in the winding, squeezing the remained superconducting area toward the outer end of the winding with an increasing propagating speed. At last, the entire coil quenches with a rapid temperature and stress rises - for some large-scale magnets, damages would occur at this moment. We consider that the effective suppression of initial turn-to-turn heat in the winding is pivotal for a future preventive approach to this kind of quench.

## V. Acknowledgments

This work was supported by the National Institute of General Medical Sciences of the National Institutes of Health under Award R01GM137138. The authors thank the support from SJTU Scholarship.

## References

[1] S. Hahn, D. K. Park, J. Bascunan, and Y. Iwasa, "HTS Pancake Coils Without Turn-to-Turn Insulation," *IEEE Transactions on Applied Superconductivity,* vol. 21, no. 3, pp. 1592-1595, Jun, 2011.

[2] R. Gyuraki, T. Benkel, F. Schreiner, F. Sirois, and F. Grilli, "Fluorescent thermal imaging of a non-insulated pancake coil wound from high temperature superconductor tape," *Superconductor Science & Technology,* vol. 32, no. 10, Oct, 2019.

[3] Y. Wang, W. K. Chan, and J. Schwartz, "Self-protection mechanisms in no-insulation (RE) Ba2Cu3Ox high temperature superconductor pancake coils," *Superconductor Science & Technology,* vol. 29, no. 4, Apr, 2016.

[4] Y. Wang, H. Song, D. Xu, Z. Y. Li, Z. Jin, and Z. Hong, "An equivalent circuit grid model for no-insulation HTS pancake coils," *Superconductor Science & Technology,* vol. 28, no. 4, Apr, 2015.

[5] Y. H. Zhai, B. Berlinger, C. Barth, and C. Senatore, "Design, construction, and testing of no-insulation small subscale solenoids for compact tokamaks," *Superconductor Science & Technology,* vol. 34, no. 10, Oct, 2021.

[6] F. Schreiner, Y. Z. Liu, Y. Z. Zhang, R. Gyuraki, M. Noe, and M. Doppelbauer, "Development of No-Insulation Racetrack Coils Wound With 2nd Generation HTS Tapes for a Stator System for Wind Generators," *IEEE Transactions on Applied Superconductivity,* vol. 30, no. 4, Jun, 2020.

[7] F. L. Dong, Z. Huang, X. F. Li, L. N. Hao, L. P. Yao, W. Wu, and Z. J. Jin, "R&D of No-Insulation HTS Magnets Using 2G Wires in a Prototype for Maglev Applications," *IEEE Transactions on Applied Superconductivity,* vol. 29, no. 5, Aug, 2019.

[8] S. Yoon, J. Kim, H. Lee, S. Hahn, and S. H. Moon, "26T 35mm all-GdBa2Cu3O7-x multi-width no-insulation superconducting magnet," *Superconductor Science & Technology,* vol. 29, no. 4, Apr, 2016.

[9] S. Hahn, D. K. Park, J. Voccio, J. Bascunan, and Y. Iwasa, "No-Insulation (NI) HTS Inserts for > 1 GHz LTS/HTS NMR Magnets," *IEEE Transactions on Applied Superconductivity,* vol. 22, no. 3, Jun, 2012.

[10] U. Bong, C. Im, J. Yoon, S. An, S. W. Jung, K. J. Han, and S. Hahn, "Investigation on Key Parameters of NI HTS Field Coils for High Power Density Synchronous Motors," *IEEE Transactions on Applied Superconductivity,* vol. 31, no. 5, Aug, 2021.

[11] F. L. Dong, Z. Huang, L. N. Hao, X. Y. Xu, Z. J. Jin, and N. Shao, "An on-board 2G HTS magnets system with cooling-power-free and persistent-current operation for ultrahigh speed superconducting maglevs," *Scientific Reports,* vol. 9, Aug 14, 2019.

[12] F. L. Dong, Z. Huang, X. Y. Xu, M. Y. Wang, X. Y. Teng, L. N. Hao, and Z. J. Jin, "Method and Process of Mechanical Evaluation of a 2G HTS Magnet System for Maglev Applications," *IEEE Transactions on Applied Superconductivity,* vol. 30, no. 4, Jun, 2020.

[13] S. Hahn, K. Kim, K. Kim, X. B. Hu, T. Painter, I. Dixon, S. Kim, K. R. Bhattarai, S. Noguchi, J. Jaroszynski, and D. C. Larbalestier, "45.5-tesla direct-current magnetic field generated with a high-temperature superconducting magnet," *Nature,* vol. 570, no. 7762, pp. 496-+, Jun 27, 2019.

[14] Y. Iwasa, and S. Hahn, "First-cut design of an all-superconducting 100-T direct current magnet," *Applied Physics Letters,* vol. 103, no. 25, Dec 16, 2013.

[15] Y. Li, and S. Roe, "Key designs of a short-bore and cryogen-free high temperature superconducting magnet system for 14 T whole-body MRI," *Superconductor Science & Technology,* vol. 34, no. 12, Dec, 2021.

[16] T. Wang, H. Quan, L. Chen, K. Z. Ding, S. S. Du, and C. L. Zou, "Conceptual Design of 3-T All HTS MRI Using No-Insulation Winding Technology: Electromagnetic Stress Reinforced Structure," *IEEE Transactions on Applied Superconductivity,* vol. 31, no. 8, Nov, 2021.

[17] K. R. Bhattarai, K. Kim, K. Kim, K. Radcliff, X. B. Hu, C. Im, T. Painter, I. Dixon, D. Larbalestier, S. Lee, and S. Hahn, "Understanding quench in no-insulation (NI) REBCO magnets through experiments and simulations," *Superconductor Science & Technology,* vol. 33, no. 3, Mar, 2020.

[18] Y. Li, D. Park, Y. F. Yan, Y. Choi, J. Lee, P. C. Michael, S. W. Chen, T. M. Qu, J. Bascunan, and Y. Iwasa, "Magnetization and screening current in an 800 MHz (18.8 T) REBCO nuclear magnetic resonance insert magnet: experimental results and numerical analysis," *Superconductor Science & Technology,* vol. 32, no. 10, Oct, 2019.

[19] Z. L. Zhang, B. Z. Zhou, J. H. Liu, L. Wang, and Q. L. Wang, "Engineering-based design and fabrication procedure for mid-

temperature REBCO magnets accommodating the strong Ic anisotropy," *Superconductivity,* vol. 1, pp. 100005, 2022.

[20] Z. Jiang, H. Song, W. Song, and R. A. Badcocka, "Optimizing coil configurations for AC loss reduction in REBCO HTS fast-ramping magnets at cryogenic temperatures," *Superconductivity,* vol. 3, pp. 100024, 2022.

[21] D. Park, J. Bascunan, Y. Li, W. Lee, Y. Choi, and Y. Iwasa, "Design Overview of the MIT 1.3-GHz LTS/HTS NMR Magnet with a New REBCO Insert," *IEEE Transactions on Applied Superconductivity,* vol. 31, no. 5, Aug, 2021.

[22] S. Noguchi, "Electromagnetic, Thermal, and Mechanical Quench Simulation of NI REBCO Pancake Coils for High Magnetic Field Generation," *IEEE Transactions on Applied Superconductivity,* vol. 29, no. 5, Aug, 2019.

[23] P. C. Michael, D. Park, Y. H. Choi, J. Lee, Y. Li, J. Bascunan, S. Noguchi, S. Hahn, and Y. Iwasa, "Assembly and Test of a 3-Nested-Coil 800-MHz REBCO Insert (H800) for the MIT 1.3 GHz LTS/HTS NMR Magnet," *IEEE Transactions on Applied Superconductivity,* vol. 29, no. 5, Aug, 2019.

[24] D. Park, J. Bascunan, P. C. Michael, J. Lee, Y. H. Choi, Y. Li, S. Hahn, and Y. Iwasa, "MIT 1.3-GHz LTS/HTS NMR Magnet: Post Quench Analysis and New 800-MHz Insert Design," *IEEE Transactions on Applied Superconductivity,* vol. 29, no. 5, Aug, 2019.

[25] B. Y. Shen, F. Grilli, and T. Coombs, "Overview of H-Formulation: A Versatile Tool for Modeling Electromagnetics in High-Temperature Superconductor Applications," *IEEE Access,* vol. 8, pp. 100403-100414, 2020.

[26] R. C. Mataira, M. D. Ainslie, R. A. Badcock, and C. W. Bumby, "Finite-element modelling of no-insulation HTS coils using rotated anisotropic resistivity," *Superconductor Science & Technology,* vol. 33, no. 8, Aug, 2020.

[27] V. M. R. Zermeno, A. B. Abrahamsen, N. Mijatovic, B. B. Jensen, and M. P. Sorensen, "Calculation of alternating current losses in stacks and coils made of second generation high temperature superconducting tapes for large scale applications," *Journal of Applied Physics,* vol. 114, no. 17, Nov 7, 2013.

[28] F. L. Dong, Z. Huang, D. R. Qiu, M. Y. Wang, A. F. Zhao, B. B. Zhu, L. B. Wang, and Z. J. Jin, "Studies on the features of characteristic resistance of a no-insulation superconducting coil in energizing and de-energizing processes," *Physica C-Superconductivity and Its Applications,* vol. 551, pp. 33-40, Aug 15, 2018.

[29] F. Dong, D. Park, W. Lee, L. Hao, Z. Huang, J. Bascunan, Z. Jin, and Y. Iwasa, "On fault-mode phenomenon in no-insulation superconducting magnets: A preventive approach," *Appl Phys Lett,* vol. 121, no. 19, pp. 194101, Nov 7, 2022.